



ARTICLE

Effects of Freeze-Thaw Cycles on Physical and Mechanical Properties of Glulam Exposed to Outdoor Environment

Ruyuan Yang¹, Haitao Li^{2,*}, Assima Dauletbek^{1,2}, Mahmud Ashraf^{2,4}, Rodolfo Lorenzo³, Youfu Sun¹ and Yuehong Wu¹

¹College of Materials Science and Engineering, Nanjing Forestry University, Nanjing, China

²College of Civil Engineering, Nanjing Forestry University, Nanjing, China

³University College London, London, WC1E 6BT, UK

⁴School of Engineering, Deakin University, Geelong, VIC 3216, Australia

*Corresponding Author: Haitao Li. Email: lhaitao1982@126.com

Received: 07 December 2020 Accepted: 06 January 2021

ABSTRACT

This paper presents an experimental investigation to identify suitable indices to assess durability of glulam when subjected to freeze-thaw cycles in an exposed environment. In this study, two types of glulam specimens were tested for their performance when subjected to different levels of aging due to freezing and thawing. Effect of aging treatment on various parameters including thickness swelling rate, static bending strength, elastic modulus, shear strength, and peeling rate of adhesive layer were studied. Obtained results showed that freeze-thaw aging treatment did not affect the water-resistance of the specimens as measured by thickness swelling rate and had little effect on the dimensional stability of the material. However, the applied aging treatment weakened the bending resistance of the glulam specimens with more pronounced effects on low-density wood. On the other hand, bond strength of high-density wood was relatively more affected due to the applied freeze-thaw cycles. For high-density wood, it is suggested that the shear strength of the adhesive layer be taken as an important index to determine the durability of freeze-thaw cycles aging. For low-density wood, on the other hand, the static bending strength can be used as an index to determine the durability of glulam under freeze-thaw cycles aging.

KEYWORDS

Freeze-thaw cycles; structural glulam; durability; wood failure percentage; accelerated aging

1 Introduction

Timber construction refers to engineering structures that use timber as the major structural system [1,2]. To overcome the limitations of using natural wood, engineered wood products have been gradually gaining popularity in construction, particularly in many developed countries around the world. Advanced wood products processing technology has promoted the development of modern timber structure [3]. With environmental sustainability becoming one of the major priorities in future construction, renewable materials like timber [4], bamboo [5–7], and other bio-composite materials [8–10] are considered in a variety of applications. Glue laminated timber (glulam) is one of the most popular and most used type of engineered wood products, in which wood laminas (usually 20 mm–45 mm in thickness) are glued



together by placing them parallel to each other along the fiber direction. Glulam can be configured according to different stress requirements whilst minimizing effects of various natural imperfections such as knots in natural wood [11,12]. Therefore, compared to the sawn timber having the same cross-sectional area, glulam has uniform moisture content, higher density, and can withstand higher bending stress. Moreover, the structure of glulam is uniform, and the internal stress is small, thus it does not crack and deform easily [13,14]. The introduction of glulam products dates back to as early as 1800, and have been in use since the Second World War [15]. In the 1940s, glulam was used in outdoor structures such as bridge engineering [16,17].

In order to ensure the safety of timber structures, the performance of wood components in different outdoor exposures has been widely investigated. Dhima et al. [18] studied the effect of temperature on the shear strength of glulam; their experimental results showed that the shear strength of glulam decreased with the increase of temperature. The moisture content of glulam after high-temperature treatment did not affect its shear strength, but it changed the mode of shear failure. Ayrimis et al. [19] studied the mechanical properties of artificial wood panels under snow loads and low temperatures when used for roofing. Drake et al. [20] evaluated the effects of subfreezing temperatures and moisture content on the shear behavior of glulam beams, they found that the strengths of the beams and their stiffnesses were observed to increase with decreasing temperature, with these effects being more pronounced in the higher moisture content beams. Francis et al. [21] investigated the bonding property changes of glulam beams treated with chromium copper arsenic (CCA) aqueous preservative in different environment and reported that CCA anti-corrosion treatment and outdoor exposure would reduce the bonding shear strength of glulam. Senalik et al. [22] studied the effects of artificial accelerated aging on the physical properties and preservative retention rate of pretreated structural plywood. Luo et al. [23] used four types of artificial accelerated aging methods to treat the southern pine glulam glued with one-component polyurethane and found that hygrothermal aging method, i.e., the “Boil test” suggested by BS EN 1087-1 [24], was the most suitable for investigating the durability of glulam. Que et al. [25] assessed the effect of salt on the shear strength along the grain of glulam strengthened with carbon fiber reinforced polymer (CFRP) and observed that the shear strength along the grain of glulam could be reduced by salt solution and alternate wetting and drying making glulam unsuitable to be used in high salinity areas. Szmurku et al. [26] found that rapid cooling had little effect on mechanical properties, while slow cooling significantly reduced the mechanical properties of wood. They also reported that the mechanical properties of wood in the natural environment were adversely affected due to the multiple freeze-thaw cycles.

Glulam structures are widely used in many parts of the world with varying climatic conditions [27]. In currently available literature, the effect of high temperature on the mechanical properties of wood has been more mature [28,29], but research on the effect of low temperature on mechanical properties of wood are relatively limited. Considering Northeast China as an example, where the average temperature in winter could reach -20°C , especially in the near water area, glulam structures will be more often subjected to alternating cycles of wetting, cooling, freezing, and dissolving. This repeated freeze-thaw process brings severe challenges to glulam members. In order to determine the impact of exposure to freezing and snow melting environment, it is necessary to evaluate the durability of glulam under freeze-thaw cycles in an outdoor environment.

2 Experimental Investigations

2.1 Materials Used for Manufacturing Glulam Specimens

According to ANSI A190.1-2012 “Standard for wood products-Structural glued laminated timber” [30] and the actual production and application of glulam in the market, two representative coniferous species, i.e., *Larix gmelinii* and *Pinus sylvestris* were selected due to their wider use in construction. These two species have their origin in Greater Khingan Mountains in Northeast China and offer considerable difference in

density making them suitable for the current investigation relevant material indices such as moisture content, air-dry density were tested following GB/T 1931-2009 [31] and GB/T 1933-2009 [32], respectively, and the test results are shown in Tab. 1. The glulam used in the current study was made of two-layer laminations of the same-grade composition with lumber dimensions of 1700 mm × 50 mm × 40 mm (length × width × height).

Table 1: Basic properties of *Larix gmelinii* and *Pinus sylvestris*

Wood species	Air-dried density (kg m ⁻³)	Moisture content (%)	Specimen size (mm)	Number of specimens
<i>Larix gmelinii</i>	0.66	10.84	20 × 20 × 20	30
<i>Pinus sylvestris</i>	0.40	11.09	20 × 20 × 20	30

Water-proof, weather-resistant phenol-resorcinol-formaldehyde resin adhesive was used in the current study; Tab. 2 shows the relevant performance indices for this adhesive. GB/T 26899-2011 “Structural glued laminated timber” [33] clearly states that resorcinol resin and phenol-resorcinol resin can be used as adhesives for lamination direction and width direction of laminations in the most severe operating conditions 3 (the components are completely exposed to the outdoor atmosphere). During the process of gluing, the mass ratio of the main agent to the curing agent was 5:1, one-sided spreading at a rate of 300 g m⁻² was used, and the opening time was approximately 35 min at 20°C. The gluing pressure used for *Larix gmelinii* and *Pinus sylvestris* were 1 MPa and 0.8 MPa, respectively, and the lamination time was 3 h. To ensure sufficient bond strengths were achieved, tests were conducted after 7 days of curing.

Table 2: Performance index of PRF

Composition	Model	Appearance	Viscosity (Pa·s)	Solid content (%)	pH	Water solubility (magnification)
Main agent	PR-1HSE	Reddish-brown viscous liquid	15	65	7.5	>5
Curing agent	PRH-10A	White powder	–	–	–	–

2.2 Experimental Techniques

2.2.1 Key Indices to Evaluate Durability against Freeze-Thaw Aging Process

Thickness swelling ratio due to freeze-thaw aging process and subsequent immersion in water, static bending strength and elastic modulus, shear strength, and peeling rate of the adhesive layer were selected as key indices to assess the durability of the specimens and the techniques used to determine those key indices are as follows:

(1) Thickness swelling rate

The thickness swelling ratio may be used to quantify the effect of moisture on the dimensional stability of glulam members [34]. Following relevant guidelines suggested in GB/T 17657-2013 “Test methods of evaluating the properties of wood-based panels and surface decorated wood-based panels” [35], the dimensions of the specimens were designed as 75 mm × 50 mm × 40 mm (length × width × height). The determination process involved following steps-1) The specimens were placed in an environment with temperature (T) = (20 ± 2)°C, relative humidity (RH) = (65 ± 5)%, until the mass was constant; at that stage the thickness (h_1) of the central point of the specimen was measured with a micrometer with a

division value of 0.01 mm; 2) The specimens were immersed in clear water with $T = (20 \pm 1)^\circ\text{C}$ and $\text{pH} = 7 \pm 1$ for 24 h. The top surface of the specimens was perpendicular to the water surface, and the distance between the specimens, between the specimens and the bottom, and the walls of the tank was at least 15 mm. The upper part of the specimens was (25 ± 5) mm lower than the water surface so that it could expand freely; 3) when the specimens were taken out of the water tank after 24 h, the water was wiped off the surface of the specimens, and the thickness (h_2) was measured at the original measuring point within 10 min. Thickness swelling ratio (TS) of glulam due to water absorption may be calculated by Eq. (1):

$$TS = \frac{h_2 - h_1}{h_1} \times 100\% \quad (1)$$

(2) Static bending strength and elastic modulus

The static bending strength and elastic modulus were determined following GB/T 26899-2011 [22], and the specimen dimensions were designed as 500 mm × 50 mm × 20 mm (length × width × height) with a span of 350 mm; the test arrangement is shown in Fig. 1. The bending test was carried out with three-point bending using a displacement controlled loading rate of 5 mm min⁻¹.

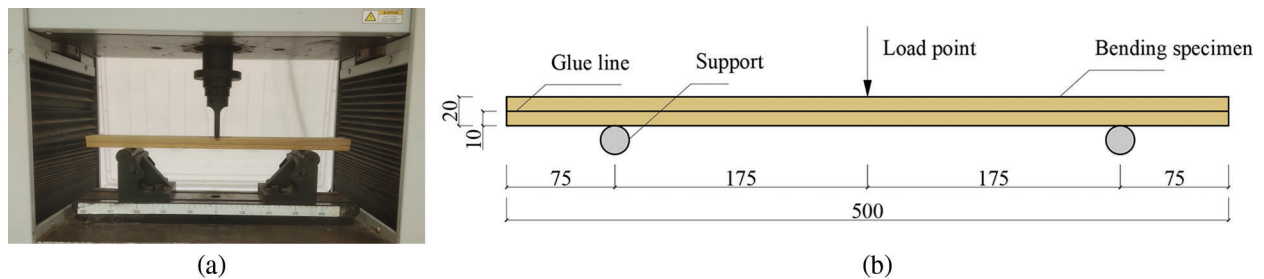


Figure 1: Three-point bending test arrangement and specimen size (all dimensions are in mm) (a) Set up used for bending test (b) Specimen size

Within the elastic range, the deflection difference between the initial load and the final load was measured, and the elastic modulus (MOE) may be calculated by Eq. (2). According to the maximum load before failure, the static bending strength (MOR) may be calculated using Eq. (3):

$$MOE = \frac{\Delta P l^3}{4bh^3 \Delta y} \quad (2)$$

$$MOR = \frac{3Pl}{2bh^2} \quad (3)$$

where ΔP denotes the difference between the upper and the lower limits of the load within the elastic range (N); l denotes the span of the bending specimen (mm); b denotes the width of the specimen (mm); Δy denotes the mid-span deflection corresponding to ΔP (mm); P denotes the maximum load at the loading point (N).

(3) Shear strength of the adhesive layer

The shear strength test of the adhesive layer was conducted according to ASTM D905-08 (2013) “Standard test methods of static tests of lumber in structural size” [36]. The test was conducted using a microcomputer-controlled electro-hydraulic servo tester with the actuator offering a maximum thrust of 30 kN. The loading speed was 5 mm/min. The wood failure percentage of each specimen was recorded after the test. The shear strength of the adhesive layer (f_v) may be calculated according to Eq. (4):

$$f_v = \frac{P_{\max}}{bl} \quad (4)$$

where P_{\max} denotes the maximum failure load (N); b denotes the width of the shear plane (mm); l denotes the length of the shear plane (mm).

(4) Peeling rate of the adhesive layer

The peeling test was carried out according to CB/T 26899-2011 [22], and the specimen size was taken as 75 mm × 50 mm × 40 mm (length × width × height) (Fig. 2). The test was divided into immersion peel test and boiling peel test. In the immersion peel test, the specimens were immersed in 10°C–15°C water for 24 h, then put into a constant temperature dryer with $T = (70 \pm 3)^\circ\text{C}$, and dried to 100%–110% of the mass before the test. Glulam members were exposed to the outdoor conditions for a long time to meet the requirements of environmental conditions 3 as specified in the standard, and hence, the aforementioned treatment was carried out twice before peeling tests were conducted. After the test, the peeling length of the adhesive layer on both ends of the specimens was measured, the total peeling rate of the two top surfaces (P) and the maximum peeling rate of the single adhesive layer (P_s) can be calculated according to Eqs. (5) and (6):

$$P = \frac{L_p}{2L} \times 100\% \quad (5)$$

$$P_s = \frac{L_{\max}}{L} \times 100\% \quad (6)$$

where L_p denotes the sum of peeling length of the adhesive layer on both ends (mm); L denotes the length of the adhesive layer on the end surface (mm). When determining the peeling length, the damage of wood due to dry crack and/or knot was not included in the peeling failure.

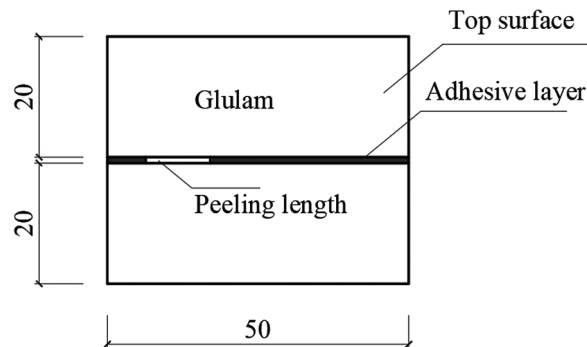


Figure 2: Peeling specimen size (all dimensions are in mm)

In the boiling peel test, the specimens were immersed in boiling water for 4 h, then kept at water at 10°C–15°C for 1 h. The specimens were taken out from the water and put into a constant temperature dryer with $T = (70 \pm 3)^\circ\text{C}$, and dried to 100%–110% of the mass before the test. During the drying process, the distance between the specimens should be at least 50 mm, and the cross-section of the wood should be parallel to the direction of airflow. To meet the requirements of operating environment 3, the above treatment process was also carried out twice. The measurement and calculation method of peeling rate were the same as those adopted for the immersion peel test.

2.2.2 Freeze-Thaw Cycles Aging Treatment Method

The equipment used in freeze-thaw cycles aging test are as follows: Mechanical universal test analyzer (Model: AG-IC 100 kN; UTM4304); electric constant temperature water tank (Model: DK-600B);

electro-thermostatic blast oven (Model: OH6-914385-II; DGG-9070B); freezer (Model: Midea BCD-135); temperature and humidity regulating box; electronic balance (accurate to 0.001g); electronic digital caliper (accurate to 0.01 mm); pH test pen (accurate to 0.01); and temperature and humidity meter.

At present, there is no specific standard for the structural glulam subjected to freeze-thaw cycles. Considering the winter average temperature in Northeast China and the actual test conditions, the freeze-thaw cycles aging treatment method, the following steps were applied in the current investigation:

- (1) The specimens were immersed in water with $T = (20 \pm 3)^{\circ}\text{C}$ and $\text{pH} = 7 \pm 0.5$ for 48 h;
- (2) After immersion, the specimens were taken out from the water, and the surface moisture was dried using a cotton cloth, and then immediately put into the freezer with $T = (-20 \pm 3)^{\circ}\text{C}$ for (8 ± 0.5) h;
- (3) After the specimen was taken out of the freezer, it was immediately immersed in water with $T = (20 \pm 3)^{\circ}\text{C}$ and $\text{pH} = 7 \pm 0.5$ for (8 ± 0.5) h;
- (4) Steps 2–3 were repeated for the next freeze-thaw cycles. The total time for each freeze-thaw cycle was (16 ± 1) h;
- (5) Every aging period consisted 7 freeze-thaw cycles, and the water in the test chamber was replaced after each period;
- (6) The test was carried out for three aging periods. At the end of each period, the specimens were placed in the environment of $T = (20 \pm 3)^{\circ}\text{C}$ and $\text{RH} = (65 \pm 5)\%$. The properties of the specimens were measured once the mass of each specimen was 100%–110% of that before the test.

In this study, two types of glulam specimens were treated by freeze-thaw cycles aging. Experimental results were carefully analyzed to study the changes in thickness swelling rate, static bending strength, elastic modulus, shear strength, and peeling rate of the adhesive layer due to the aging treatment. This investigation suggests some indices for glulam produced from high and low density wood that could be used to assess durability against freeze-thaw cycles. A total of 320 specimens were tested in 2 groups as part of the current study. After the completion of each aging period, 10 specimens from each wood species were selected to be tested to evaluate key indices (Note: Due to the limitation of test conditions, the specimens for testing the peeling rate of the adhesive layer were also used to test the thickness swelling rate). To reduce the error, the average values were used in the study.

3 Test Results and Discussion

3.1 Effect of Freeze-Thaw Cycles on Specimens

The specimens under freeze-thaw cycles were carefully inspected to understand the effects of simulated extreme weathering conditions. However, it was found that the freeze-thaw cycles had little effect on the shape and the appearance of the specimens. At the end of aging, small cracks occurred in the direction of annual rings as shown in Fig. 3. The cracks of individual *Larix gmelinii* specimens typically appeared at the boundary of early and late wood, whilst some specimens with knots cracked around the knots. Overall, the considered specimens did not suffer any significant obvious failure due to exposure to the applied freeze-thaw cycles.

3.2 Thickness Swelling Due to Water Absorption

Thickness swelling was measured at two stages to investigate the effect of freeze-thaw cycles on glulam's durability. At the first stage, thickness swelling was measured after three periods of freeze-thaw cycles aging treatment. Once these measurements were done, all specimens were immersed in water for 24 h and the second thickness swelling was measured to see the effect of freeze-thaw aging on water absorption. Tab. 3 shows the mean and COVs of measured thickness values and corresponding thickness swelling rates for all considered specimens. As observed from Tab. 3, aging treatment increased the

thickness of both types of glulam specimens considered in the current study as. The aging process caused some damage to the adhesive and wood surface, which led to swelling due to water absorption. However, the thickness swelling rate of the specimens was less than 3.5%, which met the requirements of of Japanese standard (<12%) JIS A 5908-2003 [37], indicating that the water-resistance of the specimens was within acceptable limit even after the extreme aging treatment. Pilarski et al. [38] carried out freeze-thaw cycles treatment on PVC/wood-flour composites with different wood species, and after five freeze-thaw cycles, and reported that the width and the thickness changed less than 1.3% and 2.2%, respectively; He et al. [39] investigated freeze-thaw cycles treatment on timber columns, and did not observe any obvious change on the surface of the considered specimens. The current study also shows that freeze-thaw cycles treatment has little effect on the dimensional stability of glulam.



Figure 3: End surfaces of considered species after exposure to freeze-thaw cycles (a) *Larix gmelinii* specimens (b) *Pinus sylvestris* specimens

Table 3: Thickness swelling rate of specimens after considered aging process

Wood species	Thickness before aging, h_1 (mm)	Thickness after aging, h_2 (mm)	Swelling rate, $(h_2-h_1)/h_1$ (%)	24 h water absorption thickness, h_3 (mm)	Swelling rate, $(h_3-h_2)/h_2$ (%)
<i>Larix gmelinii</i>	39.66 (0.0069)	40.94 (0.0042)	3.23 (0.1321)	41.39 (0.0054)	1.10 (0.1414)
<i>Pinus sylvestris</i>	39.60 (0.0037)	40.40 (0.0218)	2.02 (0.1520)	40.71 (0.0203)	0.77 (0.1691)

Note: The data in the table are the average values of test data after three freeze-thaw cycles aging, and the value within brackets are the corresponding coefficient of variation.

The thickness swelling rate due to freeze-thaw cycle aging and that after 24 h water immersion for *Larix gmelinii* specimens were higher than those of *Pinus sylvestris* as shown in Fig. 4. The reason for the difference in swelling may be that the dry shrinkage (wet expansion) rate of *Larix gmelinii* is higher than that of *Pinus sylvestris*. The thickness swelling rate at 24 h water immersion of the two specimens was lower than that after aging, which is due to the release of internal growth and bonding stress during the continuous freeze-thaw cycles.

3.3 Analysis of Static Bending Strength and Elastic Modulus

Fig. 5 shows the observed trends in change of flexural properties for the considered glulam specimens under various stages of freeze-thaw cycles. It is obvious that with the increase of aging periods, the static bending strength and the elastic modulus of both types of specimens showed gradual deterioration. Previous research on wood-plastic composite (WPC) [40,41] also reported similar effect of freeze-thaw cycles on bending properties of WPC. They also reported that the flexural properties of WPC depend on

the melting temperature; higher melting temperature resulted in reduced static bending strength and elastic modulus of the specimens. Both glulam and WPC are wood-based composite materials, but their material properties are different. Glulam is made by gluing laminations with adhesives; its strength depends on the type of wood as well as the bonding strength between layers. In the process of freeze-thaw cycles, the mechanical properties of wood and resin decreased, and the stress transfer between laminations was directly affected, which eventually weakened the bending performance of the specimens.

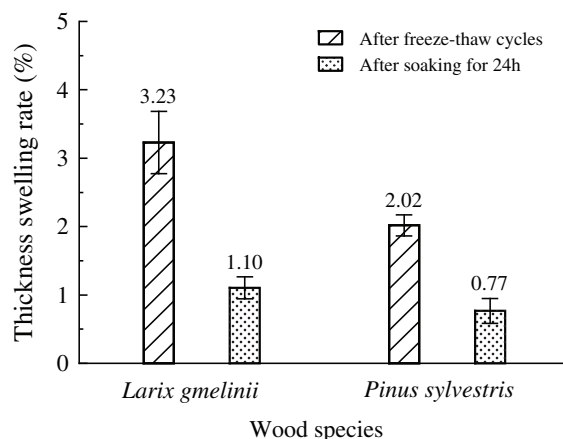


Figure 4: Comparison of the thickness swelling rate of different wood species after freeze-thaw cycles and after immersion in water for 24 h

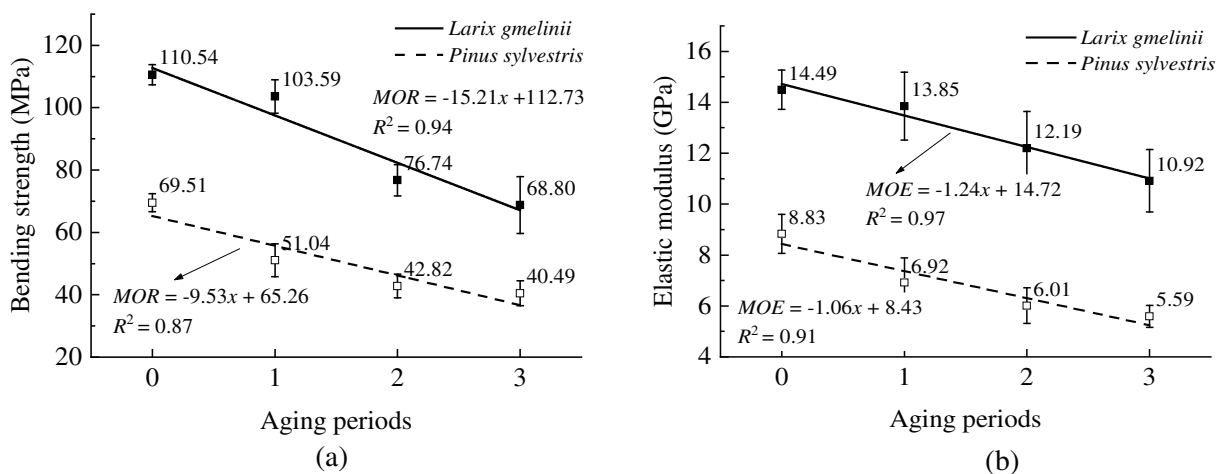


Figure 5: Static bending strength and elastic modulus after freeze-thaw cycles aging treatment (a) Static bending strength (b) Elastic modulus

Note: Aging period 0 denotes the specimen without deterioration.

For *Larix gmelinii* specimens, the loss of static bending strength and elastic modulus was the largest during the second stage of aging treatment. After 3 cycles of aging, the static bending strength and elastic modulus decreased by a total of 37.8% and 24.6%, respectively. The loss of static bending strength and elastic modulus for *Pinus sylvestris* specimens was the largest during the first stage of aging treatment. Overall, after 3 cycles of aging, *Pinus sylvestris* suffered higher deterioration in bending properties when compared against those of *Larix gmelinii*; the static bending strength and the elastic modulus of *Pinus*

sylvestris decreased by 41.7% and 36.7%, respectively. After the end of aging cycles, some bending specimens of *Pinus sylvestris* cracked at the nodes, which somewhat explains the low retention rate of flexural properties of *Pinus sylvestris* specimens.

3.4 Analysis of Shear Strength and Peeling Rate of the Adhesive Layer

According to the requirements of GB/T 26899-2011 [22] regarding the shear strength of adhesive layer and percentage of wood failure, at a moisture content of 8%–15%, it is required that the average shear strength is at least 6.0 MPa, whilst the average wood failure percentage is at least 144-(9 f_v), and the minimum single value of wood failure percentage is 153.3-(13.3 f_v), where f_v denotes the shear strength of adhesive layer (MPa). According to the minimum requirement of gluing capacity for structural glulam structure in GB/T 50329-2012 “Standard for test methods of timber structures” [42], the shear strength of the adhesive layer along the grain of *Pinus koraiensis* and other soft pine specimens is 5.9 MPa in the dry state. If the strength of the specimen is lower than the specified value, but the wood failure percentage is not less than 75%, the specimen can still be considered as suitable for use. Fig. 6 presents the shear strength parameters measured from tests conducted on the considered glulam specimens. From the test results of untreated samples (aging period 0), it can be seen that the shear strength and percentage of wood failure of the two specimens in a dry state meet the minimum requirements of the relevant standards.

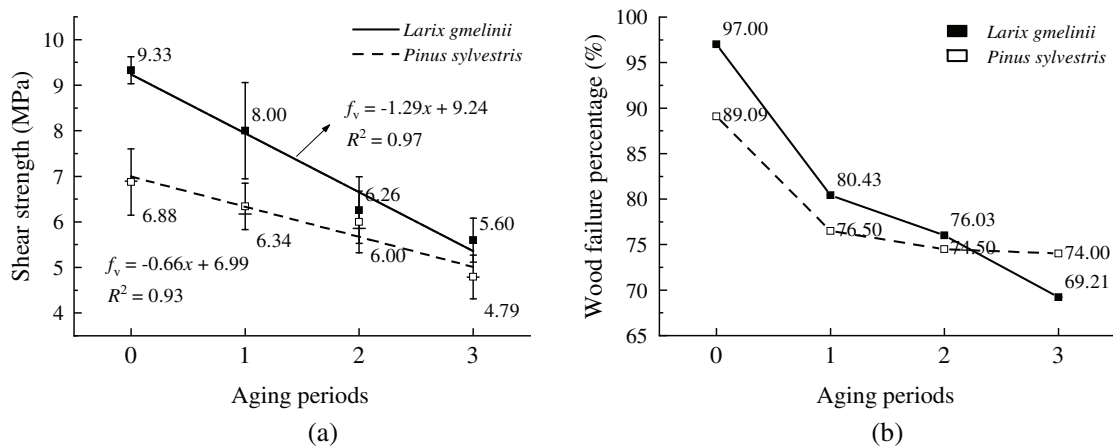


Figure 6: Shearing strength of specimens after the accelerated aging process (a) Shear strength of the adhesive layer (b) Wood failure percentage

Note: Aging period 0 denotes the specimen without deterioration.

Observed changes in shear strength of the adhesive layer of *Larix gmelinii* and *Pinus sylvestris* specimens after freeze-thaw cycles aging treatment are shown in Fig. 6. With the increase of aging periods, the shear strength of both types of glulam specimens showed a downward trend. At the end of the first and the second stages of freeze-thaw cycles, a small amount of resin was observed on the end surface of *Larix gmelinii* specimens, which somewhat explains the rapid decrease of bonding strength of *Larix gmelinii* specimens. At the end of the three aging stages, the shear strength of the *Larix gmelinii* specimens decreased by 40.0% compared with that of the untreated specimen, and the wood failure percentage decreased to 69.2%. Whereas, the shear strength of the *Pinus sylvestris* decreased by 30.4% and the wood failure percentage decreased to 74.0%. It can be seen that the effect of freeze-thaw cycles aging treatment on the shear strength of *Larix gmelinii* specimens is greater than that of *Pinus sylvestris*. This observed variation may have been caused by the difference of density between earlywood and latewood of *Larix gmelinii*, and by the the internal stresses caused by uneven wet swelling inside the wood, which affected the bonding strength due to the continuous change of external temperature.

Experimental research conducted by Wu [43] showed that the internal stresses caused by the change of moisture content in wood with high density is greater than those of wood with low density. For the same adhesive, the bonding durability of high-density wood is worse than that of low-density wood.

According to the requirements of GB/T 26899-2011 [22] for the peeling rate of the adhesive layer, the total peeling rate of the specimens should be less than 5%, and the maximum peeling length of any adhesive layer should not be greater than 1/4 of the adhesive layer length. Tab. 4 lists the measured key indices for peeling and the results showed that the peeling rate of the specimens without degradation meets the requirements of relevant standards. The test results of immersion peeling rate and boiling peeling rate of specimens after each aging stage are shown in Tab. 4. With the increase of aging periods, the peeling rate of the adhesive layer of the considered two specimen types increased gradually. After two cycles of peeling, the total stripping rate of *Larix gmelinii* specimens was 26.1%, and the maximum peeling rate of the single adhesive layer reached 100%, while those of *Pinus sylvestris* was 8.6% and 62.6%, respectively. It should be noted that the boiling peeling rate of the two specimen types after freeze-thaw cycles aging treatment was less than that of the immersion peeling. Water boiling treatment eliminated the internal stress caused by the long-term freeze-thaw cycles, and thus may have contributed to the reduced peeling rate of the adhesive layer.

Table 4: Peeling rate of the adhesive layer after freeze-thaw cycles aging treatment

Wood species/peeling mode		Aging period	Single peeling		Two-cycle peeling	
			P (%)	P_s (%)	P (%)	P_s (%)
<i>Larix gmelinii</i>	Immersion peeling	0	0	0	0.64	2.81
		1	10.76	22.37	15.58	41.10
		2	13.71	100	18.87	100
		3	19.43	100	26.13	100
	Boiling peeling	0	0	0	2.73	8.40
		1	3.16	10.52	5.30	21.73
		2	9.74	22.14	14.67	47.89
		3	18.69	34.62	25.17	51.34
<i>Pinus sylvestris</i>	Immersion peeling	0	0	0	0	0
		1	0	0	3.79	45.50
		2	2.68	19.13	5.21	62.57
		3	4.42	24.51	8.64	51.32
	Boiling peeling	0	0	0	0	0
		1	0	0	0	0
		2	0	0	3.17	18.54
		3	2.83	18.00	4.00	24.20

Note: Aging period 0 denotes the specimen without deterioration; P denotes the total peeling rate of the two end surfaces (%); P_s denotes the maximum peeling rate of the single adhesive layer (%)

3.5 Observed Changes in Performance of Specimens after Aging Treatment

The above test results show that the changes in performance of different wood species are different after aging treatment. To assess the observed changes, the performance of the untreated specimen was considered

as 100%, and the retention rate of various parameters at different stages of aging were used for relevant comparisons in the current study. As shown in Section 3.2, thickness swelling indices after aging treatment as well as after 24 h water immersion were less than 3.5%. This clearly shows that the thickness swelling index can not be used to appropriately evaluate the durability of glulam against freeze-thaw aging process. Fig. 7 compares the retention of bending properties and shear strength for the two types of specimens after freeze-thaw cycles aging treatment. For *Larix gmelinii* specimens (see Fig. 7a), the shear strength of the adhesive layer decreased the most, by 37.8% after the aging treatment, whereas *Pinus sylvestris* specimens (see Fig. 7b) were more vulnerable against bending showing a reduction of 41.8% in static bending strength. It was observed that wood density has a clear impact on the durability of wood during freeze-thaw cycles. For high-density wood, the freeze-thaw cycles process has a greater impact on the bonding interface. It is suggested that the shear strength of the adhesive layer should be taken as an important index to determine the durability of wood during freeze-thaw cycles aging; whereas for low-density wood, the static bending strength can be used as a suitable index. However, the effect of wood density on freeze-thaw aging process should be evaluated using larger sample sizes offering wider variations in density in future research.

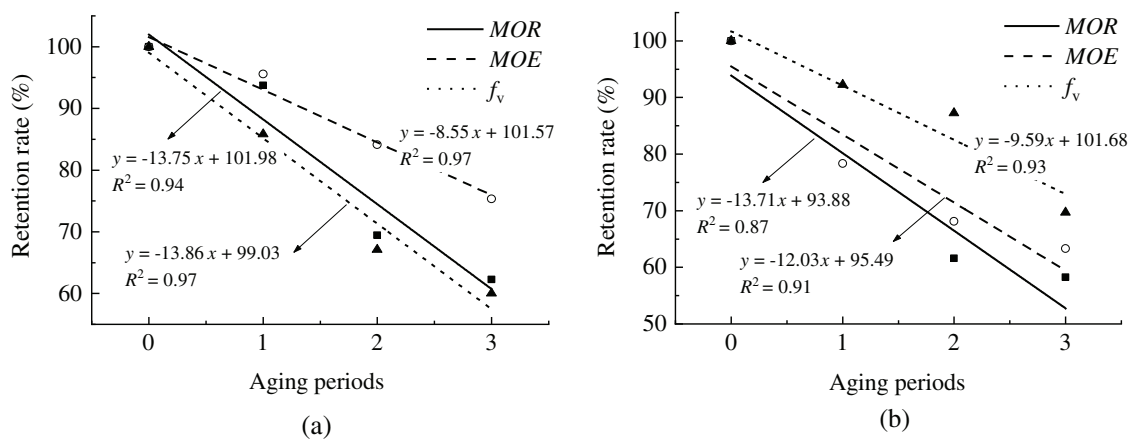


Figure 7: Performance changes of specimens after freeze-thaw cycles aging treatment (a) *Larix gmelinii* specimens (b) *Pinus sylvestris* specimens

3.6 Variance Analysis of Mechanical Properties under Freeze-Thaw Cycles

In order to analyze the influence of the aging period and the wood species under freeze-thaw cycles aging treatment on its bending strength (MOR), elastic modulus (MOE) and shear strength of the adhesive layer (f_v), the test data were analyzed by variance analysis of randomized block design. When the MOR and MOE were analyzed, at the level of $\alpha = 0.05$, significant level of the effect of the aging periods are 0.047 and 0.005, respectively, and significant level of the wood species are 0.020 and 0.000, respectively. In order to better discuss the influence of aging periods and wood species on f_v , the test level was expanded. The level of $\alpha = 0.10$ was adopted, which can improve the test efficiency. The change of f_v was discussed within 90% confidence interval, and the accuracy of the analysis results was improved. At the level of $\alpha = 0.10$, significant level of the effect of the aging periods and the wood species are both 0.075. Variance analysis results are shown in Tab. 5, it can be seen that the different levels of aging periods and wood species have significant on the three mechanical properties.

Table 5: Variance analysis of three mechanical properties

Mechanical properties	Source	SS	df	MS	F-value	Significant
<i>MOR</i>	Intercept	39660.38	1	39660.38	13.08	0.172
		3031.26	1	3031.26		
	Aging periods	1578.47	3	526.16	9.64	0.047
		163.69	3	54.56		
	Wood species	3031.26	1	3031.26	55.56	0.005
		163.69	3	54.56		
<i>MOE</i>	Intercept	7.76×10^8	1	7.76×10^8	10.71	0.189
		7.25×10^7	1	7.25×10^7		
	Aging periods	1.33×10^7	3	4.44×10^6	18.34	0.020
		7.26×10^5	3	2.42×10^5		
	Wood species	7.25×10^7	1	7.25×10^7	299.55	0.000
		7.26×10^5	3	2.42×10^5		
<i>f_v</i>	Intercept	205.57	1	205.57	105.59	0.062
		1.95	1	1.95		
	Aging periods	5.50	3	1.83	6.76	0.075
		0.81	3	0.27		
	Wood species	1.95	1	1.95	7.18	0.075
		0.81	3	0.27		

4 Conclusions

320 glulam specimens manufactured from 2 types of wood species, i.e., *Larix gmelinii* and *Pinus sylvestris* were used in the current study to investigate the effect of freeze-thaw cycles on durability. Based on test results and subsequent analysis, the following conclusions can be drawn:

1. Continuous changes in temperature and humidity during the freeze-thaw cycles showed insignificant effect on the water absorption behavior of glulam; the thickness swelling rate was less than 3.5%, which seemed to indicate that glulam specimens met the requirements of relevant standards. It showed that the aging process due to freeze-thaw cycles had no significant effect on the dimensional stability as well as on the water-resistance ability of the glulam specimens. Hence, the thickness swelling rate should not be used a key indicator to assess the overall durability performance of glulam when subjected to freeze-thaw cycles.
2. Test results showed that freeze-thaw cycles can considerably weaken the bending performance of glulam specimens, and the influence on low-density wood is more significant when the same adhesive is used to manufacture. The shear strength of the adhesive layer for both types of specimens met relevant strength standards when subjected to freeze-thaw cycles. However, the bond strength of high-density wood was more affected than that of low-density wood.
3. Changes in mechanical properties due to the applied aging treatment were critically analyzed to find indices that can be reliably used to assess the effect of freeze-thaw cycles on glulam. For high-density wood, it is suggested that the shear strength of the adhesive layer can be taken as an important index

to determine the durability of wood during freeze-thaw cycles aging, whereas for low-density wood, the static bending strength can be used as a reliable index. However, it is worth noting that wider variations in wood specimen densities should be considered in future research to evaluate the effect of wood density on durability of glulam under freeze-thaw cycles.

4. Based on obtained test results and subsequent analysis it is obvious that freeze-thaw cycles could significantly weaken the mechanical properties of glulam. Therefore, it is suggested that some thermal insulation materials should be added outside the glulam members, and use of glulam must be carefully and thoroughly assessed prior to using for construction in places with large temperature differences.

Funding Statement: This research is supported by the Natural Science Foundation of Jiang-su Province (Grant No. BK20181402), the National Natural Science Foundation of China (Grant No. 51878354), a Project Funded by the National First-class Disciplines (PNFD), a Project Funded by the Priority Academic Program Development of Jiangsu Higher Education Institutions (PAPD), and a Project Funded by the Co-Innovation Center of Efficient Processing and Utilization of Forest Resources, Nanjing Forestry University (Nanjing, China). Any research results expressed in this paper are those of the writer (s) and do not necessarily reflect the views of the foundations.

Conflicts of Interest: The authors declare that they have no conflicts of interest to report regarding the present study.

References

1. Li, X., Ashraf, M., Li, H. T., Zheng, X. Y., Wang, H. X. et al. (2019). An experimental investigation on Parallel Bamboo Strand Lumber specimens under quasi static and impact loading. *Construction and Building Materials*, 228(9), 116724. DOI 10.1016/j.conbuildmat.2019.116724.
2. Xie, W. B., Ding, Y. W., Wang, Z., Gao, Z. Z., Zhang, T. Y. et al. (2020). Testing and analysis of hemlock cross laminated timber. *Wood Research*, 65(5), 819–832. DOI 10.37763/wr.1336-4561/65.5.819832.
3. Zhang, J. T., Wang, Z. Q., Zhao, T., Liu, Y. X., Dong, W. Q. (2020). Study on shear performance of 3-layer CLT T&G joints under monotonic loading. *Journal of Forestry Engineering*, 5(4), 67–72. DOI 10.13360/j.issn.2096-1359.201910014.
4. Shi, C. X., Yu, Y. L., Zhu, Y. Q., Liu, Y. M., Yu, M. et al. (2020). The difference of density and shrinkage properties of six cloned poplar trees. *Journal of Forestry Engineering*, 5(5), 57–62. DOI 10.13360/j.issn.2096-1359.201908010.
5. Li, H. T., Xuan, Y. W., Xu, B., Li, S. H. (2020). Bamboo application in civil engineering field. *Journal of Forestry Engineering*, 5(6), 1–10. DOI 10.13360/j.issn.2096-1359.202003001.
6. Li, H. T., Qiu, Z. Y., Wu, G., Wei, D. D., Lorenzo, R. et al. (2019). Compression behaviors of parallel bamboo strand lumber under static loading. *Journal of Renewable Materials*, 7(7), 583–600. DOI 10.32604/jrm.2019.07592.
7. He, S., Chen, Y. H., Wu, Z. X., Hu, Y. A. (2020). Research progress on wood/bamboo microscopic fluid transportation. *Journal of Forestry Engineering*, 5(2), 12–19. DOI 10.13360/j.issn.2096-1359.201906043.
8. Li, Q., Wang, Z. Q., Liang, Z. J., Li, L., Gong, M. et al. (2020). Shear properties of hybrid CLT fabricated with lumber and OSB. *Construction and Building Materials*, 261(12), 120504. DOI 10.1016/j.conbuildmat.2020.120504.
9. Li, H. T., Wu, G., Zhang, Q. S., Deeks, A. J., Su, J. W. (2018). Ultimate bending capacity evaluation of laminated bamboo lumber beams. *Construction and Building Materials*, 160(4), 365–375. DOI 10.1016/j.conbuildmat.2017.11.058.
10. Gui, T., Cai, S. C., Wang, Z. Q., Zhou, J. H. (2020). Influence of aspect ratio on rolling shear properties of fast-grown small diameter eucalyptus lumber. *Journal of Renewable Materials*, 8(9), 1053–1066. DOI 10.32604/jrm.2020.011645.

11. Yang, R. Y., Li, H. T., Lorenzo, R., Ashraf, M., Sun, Y. F. et al. (2020). Mechanical behaviour of steel timber composite shear connections. *Construction and Building Materials*, 258(6), 119605. DOI 10.1016/j.conbuildmat.2020.119605.
12. Lu, X. R., Teng, Q. C., Li, Z. R., Zhang, X. L., Wang, X. M. et al. (2020). Study on shear property of spruce glulam and steel plate connected with inclined screw. *Journal of Forestry Engineering*, 5(3), 48–53. DOI 10.13360/j.issn.2096-1359.201906005.
13. Ding, Y. W., Zhang, Y. F., Wang, Z., Gao, Z. Z., Zhang, T. Y. et al. (2020). Vibration test and comfort analysis of environmental and impact excitation for wooden floor structure. *BioResources*, 15(4), 8212–8234.
14. Fu, H. Y., Ding, Y. W., Li, M. M., Cao, Y., Xie, W. B. et al. (2020). Research and simulation analysis of thermal performance and hygrothermal behavior of timber-framed walls with different external thermal insulation layer: Cork board and anticorrosive pine plate. *Journal of Building Physics*. DOI 10.1177/1744259120936720.
15. Dong, W., Li, Q., Wang, Z., Zhang, H., Gong, M. (2020). Effects of embedment side and loading direction on embedment strength of cross-laminated timber for smooth dowels. *European Journal of Wood and Wood Products*, 78(1), 17–25. DOI 10.1007/s00107-019-01490-z.
16. Yang, R. Y., Hong, C. K., Zhang, X. F., Yuan, Q., Sun, Y. F. (2020). Experimental research on structural behaviors of glulam I-beam with a special-shaped section. *Journal of Renewable Materials*, 8(2), 113–132. DOI 10.32604/jrm.2020.08190.
17. Dong, W. Q., Wang, Z. Q., Zhou, J. H., Zhang, H., Yao, Y. et al. (2020). Embedment strength of smooth dowel-type fasteners in cross-laminated timber. *Construction and Building Materials*, 233(3), 117243. DOI 10.1016/j.conbuildmat.2019.117243.
18. Dhima, D., Audebert, M., Racher, P., Bouchaïr, A., Taazount, M. (2014). Shear tests of glulam at elevated temperatures. *Fire and Materials*, 38(8), 827–842. DOI 10.1002/fam.2226.
19. Ayırlımis, N., Buyuksari, U., As, N. (2010). Bending strength and modulus of elasticity of wood-based panels at cold and moderate temperatures. *Cold Regions Science and Technology*, 63(1–2), 40–43. DOI 10.1016/j.coldregions.2010.05.004.
20. Drake, G., Berry, M., Schroeder, D. (2015). Effect of cold temperatures on the shear behavior of glued laminated beams. *Cold Regions Science and Technology*, 112(1–2), 45–50. DOI 10.1016/j.coldregions.2015.01.002.
21. Francis, L., Ahmad, Z. (2017). Bonding performance of CCA treated glulam timber under different environmental exposure. *Journal of Engineering and Applied Sciences*, 12(16), 4047–4052. DOI 10.3923/jeasci.2017.4047.4052.
22. Senalik, C. A., Ross, R. J., Zelinka, S. L. (2017). Accelerated aging of preservative-treated structural plywood. *Research Paper, FPL-RP-691*. Madison, WI: USA. Department of Agriculture, Forest Service, Forest Products Laboratory.
23. Luo, Z. H., Cai, X. R., Zhang, J., Chen, J., Sun, Y. F. (2015). Study on bonding property and aging resistant performance of glulam members. *China Forest Products Industry*, 42(03), 18–21. DOI 10.19531/j.issn1001-5299.2015.03.005.
24. BS EN 1087-1 (1995). *Particle boards - Determination of moisture resistance-Particle boards-Determination of moisture resistance-Boil test*. British Standards Institution.
25. Que, Z. L., Teng, Q. C., Wang, F. B., Zhao, D., Ma, C. X. (2015). Effect of salinity on the shear strength with parallel grain of CFRP-reinforced glulam. *Journal of Fujian Agriculture and Forestry University (Natural Science Edition)*, 44(4), 436–441. DOI 10.13323/j.cnki.j.fafu(nat.sci.).2015.04.018.
26. Szmotku, M. B., Campean, M., Porojan, M. (2013). Strength reduction of spruce wood through slow freezing. *European Journal of Wood and Wood Products*, 71(2), 205–210. DOI 10.1007/s00107-013-0667-6.
27. Tian, L. M., Kou, Y. F., Hao, J. P. (2019). Axial compressive behaviour of sprayed composite mortar–original bamboo composite columns. *Construction and Building Materials*, 215(9), 726–736. DOI 10.1016/j.conbuildmat.2019.04.234.
28. Zhou, J. H., Hu, C. S., Hu, S. F., Yun, H., Jiang, G. F. et al. (2012). Effects of temperature on the bending performance of wood-based panels. *BioResources*, 7(3), 3597–3606. DOI 10.4067/S0718-221X2012000200010.

29. Moya, R., Fallas-Valverde, L., Berrocal, A., Mendez-Alvarez, D. (2017). Durability of thermally modified wood of *Gmelina arborea* and *Tectona grandis* tested under field and accelerated conditions. *Journal of Renewable Materials*, 5(3), 208–219. DOI 10.7569/JRM.2017.634111.
30. ANSI A190.1 (2012). *Standard for wood products-structural glued laminated timber*. ASTM International.
31. GB/T 1931 (2009). *Method for determination of the moisture content of wood*. Beijing: Standards Press of China.
32. GB/T 1933 (2009). *Method for determination of the density of wood*. Beijing: Standards Press of China.
33. GB/T 26899 (2011). *Structural glued laminated timber*. Beijing: Standards Press of China.
34. Grosse, C., Noel, M., Thevenon, M. F., Rautkari, L., Gerardin, P. (2017). Influence of water and humidity on wood modification with lactic acid. *Journal of Renewable Materials*, 6(3), 259–269. DOI 10.7569/JRM.2017.634176.
35. GB/T 17657 (2013). *Test methods of evaluating the properties of wood-based panels and surface decorated wood-based panels*. Beijing: Standards Press of China.
36. ASTM D905-08 (2013). *Standard test methods of static tests of lumber in structural size*. ASTM International.
37. JIS A 5908 (2003). *Particle board*. Tokyo: Japanese Standards Association.
38. Pilarski, J. M., Matuana, L. M. (2005). Durability of wood flour-plastic composites exposed to accelerated freeze-thaw cycling. Part I. Rigid PVC matrix. *Journal of Vinyl and Additive Technology*, 11(1), 1–8. DOI 10.1002/vnl.20029.
39. He, K., Chen, Y., Wang, J. (2020). Axial mechanical properties of timber columns subjected to freeze-thaw cycles. *Journal of Renewable Materials*, 8(8), 969–992. DOI 10.32604/jrm.2020.09573.
40. Wang, W., He, L., Dong, L. J., Sun, H. Y., Xu, B. (2013). Effect of freeze-thaw circle environment on the bending resistance of wood-plastic composites. *Jiangxi Forestry Science and Technology*, 6, 40–42. DOI 10.16259/j.cnki.36-1342/s.2013.06.003.
41. Xiao, W. (2010). *The influence of accelerated aging on the properties of wood-plastic composite materials: Freeze-thaw, xenon accelerated aging (Master Thesis)*. China: Nanjing Forestry University.
42. GB/T 50329 (2012). *Standard for test methods of timber structures*. Beijing: China Architecture & Building Press.
43. Wu, Y. H. (2020). *The study on aging resistant performance of outdoor glulam (Master Thesis)*. China: Nanjing Forestry University.